PROCEEDINGS OF SCIENCE

LASER GENERATED PLASMAS FOR NUCLEAR ASTROPHYSICAL STUDIES

N. Gambino,[ab]*, D. Mascali[a], S. Tudisco[a], A. Anzalone[a], J. Costello[c], C. Fallon[c], S. Gammino[a], P. Hayden[c], F. Musumeci[a], A. Spitaleri[a]

[a]*INFN-Laboratori Nazionali del Sud, Via S.Sofia 62, I95123 Catania Italy,*
[b]*IET-Institute of Energy Technology, LEC-Laboratory for Energy Conversion, ETH Zurich, Sonneggstrasse 3, CH-8092 Zurich, Switzerland,*
[c]*School of Physical Sciences and National Centre for Plasma Science and Technology, DCU-Dublin City University, Glasnevin, Dublin 9, Ireland*
E-mail: gambinon@ethz.ch

In this paper a review of the experimental and numerical results obtained from the investigation of the dynamic of a laser produced plasma in the nanosecond pulse regime is presented. The aim of the work is to use laser plasmas as a tool for fusions reaction rates measurements in low energy domain. These studies include the investigation of the electron screening effect on the total number of fusions. In a laser irradiance regime of $10^{12} W/cm^2$, the produced plasma ion temperatures are high enough to ensure a not negligible number of fusion events ($> 100 eV$) while clouds of cold electrons with temperatures on the order of few eV's could provide to a not negligible influence of the screening. This confers to laser plasmas the unique peculiarity to be employed for fusion reaction rates measurements in a low energy domain. For the same purposes also multiple counter-propagating colliding laser plasmas can be employed. The dynamic of a single expanding plasma was investigated with Langmuir Probe measurements. Other than the classical hydrodynamic expansion, at the early stage of the plasma expansion, the formation of Double and Multi-layers was observed. The measurements on colliding plasmas were carried out by combining time resolved imaging and spectroscopy. Fast imaging and emission spectroscopy data revealed detailed information about the dynamic of spectral emission of the atomic species which compose the colliding region of the two plumes. The overall experimental results are promising for the design of experiments devoted to fusion reaction rate measurements by including the effect of the electron screening. Numerical fusion reaction rate calculations were also carried out, in order to determine the influence of the screening on the total number of fusions.

VI European Summer School on Experimental Nuclear Astrophysics, ENAS 6
September 18-27, 2011
Acireale Italy

*Speaker.

PoS(ENAS 6)064

1. Introduction

Astrophysical studies devoted to plasma investigations cannot be improved without a fully understanding of the related physics [1]. Studies through laboratory plasmas can be related to space plasmas through scale laws. Numerical simulations already demonstrated that the classical Debye-Hückel Electron Screening (ES) in Laser Produced Plasmas (LPP's) at irradiances of about $10^{12} W cm^{-2}$ is similar to the one of the solar core [2, 3]. At these irradiances, the laser- solid target interaction, the ablation process and the subsequent plume expansion in the nanosecond pulse regime is well know [4]. However, some non linear mechanisms developing at the early stage of the plume dynamic, such as Double Layers [5] formation or emission of prompt electrons [6, 7] have still different theoretical interpretations. The measurements realized on a single expanding plasma at the LNS-INFN of Catania, permitted us to study in detail a fast particle dynamic that develops at the early stage of the plume formation. This dynamic was related to the classical hydrodynamic expansion of the bulk plasma, where a Two Electron Temperature (TET) plasma was detected [8]. Measurements on colliding plasmas were realized at the DCU, at the same laser irradiance used to produce the single expanding plume. In this low laser irradiance regime two counter-propagating plumes (called seeds), expanding at a distance of a few millimeters from each other, don't show consistently interpenetration. That means that the collisional parameter is $\xi = D/\lambda_{ii} \gg 1$, where D is the distance between the two seeds and λ_{ii} is the Spitzer mean free path [9]. At the interaction region a so-called *stagnation layer* is formed [10]. It can be studied as a third layer of plasma which electron density and electron temperature are in a range of values useful to study the electron screening [11]. The preliminary fusion reaction rate estimations show that the screening factor has a weight on the order of the 20% on determining the total number of fusions.

2. Dynamic of the single expanding laser produced plasma

2.1 Experimental Set-Up

The experimental apparatus is fully described in [3]. A ND:Yag laser operating at 600 mJ with FWHM of 1.064 μm and pulse duration of 6 ns is focused on pure Al thick targets through a plano convex lens. Spot sizes diameter was on the order of 80 μm, so that the laser irradiance was on the order of 10^{12} $W cm^{-2}$. We operated in single shot mode and at vacuum pressure levels of $1 \cdot 10^{-6}$ mbar. A movable Langmuir Probe was placed at different distances from the target surface (from 2 mm to 50 mm with steps of $2-3$ mm), parallel to the plasma expansion direction. The probe core is a 5 mm long tungsten cylindrical tip having a diameter of 0.15 mm. By biasing the probe from $-60V$ to $+60V$ the plasma current signals versus time $I(t)$ (i.e. ions and electrons are attracted on the probe surface) are obtained. Plotting the current values I versus the applied probe voltage V at different expansion times t, the so-called *I-V* curves are obtained [3]. By analyzing the I-V curves the electron temperature and the electron density versus time are obtained. Details regarding the analysis of the I-V curves can be found in [3].

2.2 Experimental Results

The current signals $I(t)$ obtained at the different probe positions (not reported here) revealed in the first 100 ns of the plume expansion a peculiar fast particle dynamics. After the laser pulse

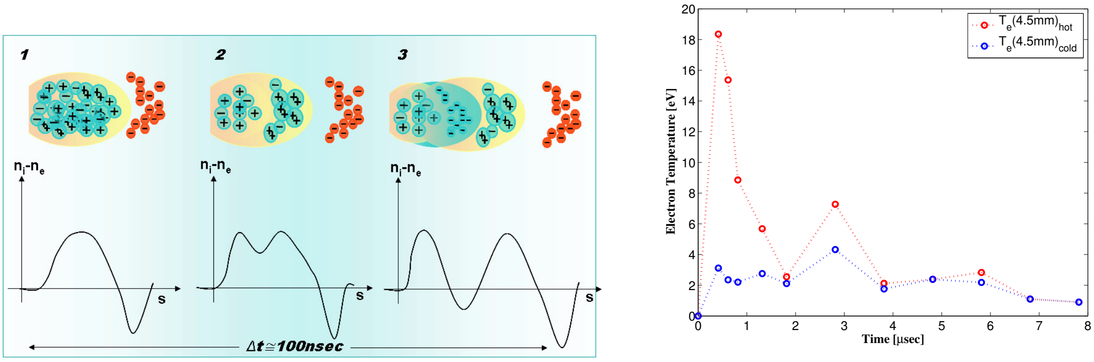

Figure 1: *ML Evolution and Electron Temperatures vs time (left) for* $d = 4.5$ *mm [8].*

ends, a fast escaping electrons group is observed at 10 ns (a first negative peak in TOF signal). They are the first charged particles that escape from the target. The first bunch is then followed by some fine structures in the positive current signal which can be interpreted as several positive ion peaks with different charge of states (i.e, an ion blow-off occurs). The fast electrons split the initial positively charged ion bunch into different, but still positive, sub-bunches (higher charge states move more rapidly). Because of the charge repulsion, the first bunches are strongly accelerated forward by the less rapid ones. When the splitting produces bunches separated by few Debye lengths $10 \simeq \lambda_D$, other groups of electrons may diffuse in the inter-bunches space accelerating also the lower charge state groups. Therefore a plurality of charged layers is formed. The multi-peak were observed until the LP was positioned at $d = 10$ mm from the target. For $d > 10$ mm the layers disappear since the transverse area of the probe is too small to "see" the flighting particles [8]. The first 100 ns of the plume expansion are therefore characterized by the expansion of a multiplicity of fast particles groups (Multi-Layers), which dynamic is summarized in figure 1 on the left [8]. They compose the coronal part of the plume, reaching as first the probe. According to data and results reported in literature, this phenomena is particular linked to the amount of energy deposited into the plasma. In the laser regime of this work it begins to assume some characteristics which are more typical of plasma generated by high laser intensity were plasma instabilities are relevant and any hydrodynamical approach fails, and only the microscopic kinetics are valid. In this regime, the dynamic is strongly non-linear and the quasi neutrality of the plume can be violated with subsequent formation of Double Layers (DL) [5]. The high laser fluence is then the principal *activator* of this dynamic. After 150 ns, the bulk plasma expansion follows, with the expected dropping density decrease. Density trends are reported in [12]: a mean value of $n_e = 1.5 \cdot 10^{18}$ m^{-3} then decreasing of one order of magnitude after $t = 5$ μs is obtained when the probe is placed at $d = 4.5$ mm from the target. Finally, at 400 ns, a hot electron tail impacts on the probe. This dynamic is favoured by the high three body recombination rate that is proportional to $T_e^{-9/2}$ [3]. On this purpose in figure 1 also the electron temperature trends are reported, obtained from the analysis of the I-V curves, when the probe was placed at $d = 4.5$ mm from the target. We revealed a Two Electron Temperature (TET) plasma, due to the simultaneous presence of a hot (T_{hot}) and a cold electron plasma population (T_{cold}). They evolve separately, starting with a temperature difference of $\Delta T = 10eV$ in the first part of the LP acquisition, then decreasing to few eVs up to 4 μs. T_{hot}

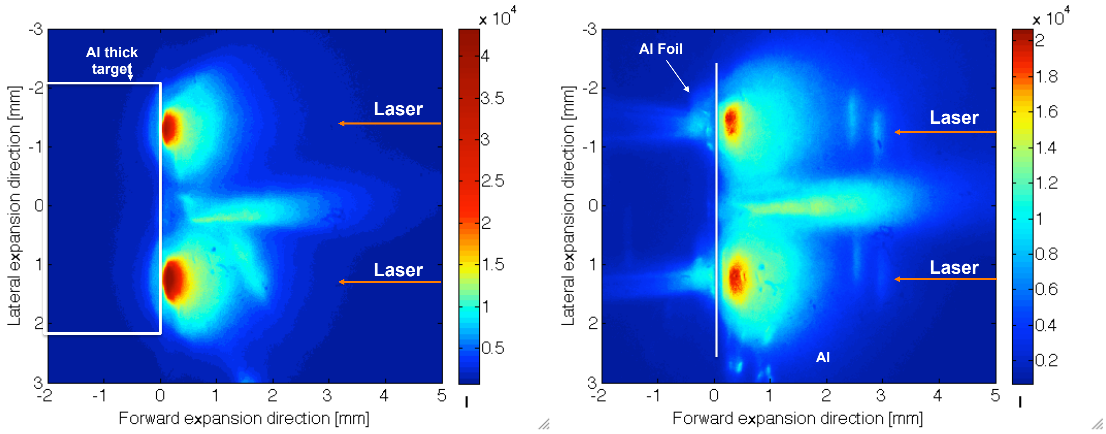

Figure 2: *Time integrating imaging of the plasma collision on the thick (left) and the thin target (right) [3].*

and T_{cold} become then comparable, because of the thermalization between the two components. It is clear from the T_{hot} trend that three recombinations are dominant in the last stage of the plume expansion. They determine the dynamic of the hot electron tail observed as last in the TOF signals [3]. The TET presence is also fundamental in order to understand the Multi Layer dynamic. When the probe was placed at $d = 14.5$ mm from the target, only a Single Electron Temperature (SET) plasma was revealed, where also no Double or Multi-Layers are detected [3]. This phenomena is related to Rarefaction of Shock Wave (RSW) that is a DL. RSW develops only for a TET plasma [5]. This phenomena is discussed in detail in [3].

3. Investigation of Colliding Plasmas

3.1 Experimental Set-Up

The experimental apparatus used to obtain the collision configuration is described in detail in [3, 11]. A Surelite III-10 Laser system operating at 600 mJ with FWHM of 1.064 μm and pulse duration of 6 ns is focused on pure Al thick targets and Al foils of $2\mu m$ of thickness through a plano convex lens. The target set-up used to achieve the plumes collision was a flat configuration [10]: an acute $\gamma = 1^\circ$ wedge prism that splits the laser beam into two parallel beams separate by a distance $D = 2.6$ mm is then focused on the Al targets. The obtained spot sizes are, for each beam, on the order of 80 μm. Each of the separate beams created by the wedge prism carries a laser energy of 300 mJ (half of the incident 600 mJ laser pulse energy). Fast imaging was spatially, spectrally and temporally resolved. It was realized with a gatable Andor ICCD camera with a 1024×1024 pixel array. It was aligned orthogonal to the plume expansion direction with an optical system described in detail in [11]. Magnification was $M = 1.62X$. Images were acquired every 5 ns, with a minimum temporal gate of 3 ns and also in time integrated mode.

3.2 Experimental Results

In figure 2 the two time integrated images report the plasma-plasma collision obtained on both thick (left) and thin (right) Al targets. In both cases the single plasmas rapidly accumulate at the centre region leading to the formation of a dense layer. This is what is called the stagnation layer, where a high collisional regime is established [10]. Time resolved images obtained on the thick targets (not reported here) show that the stagnation layer begins to form at $t = 30ns$. Therefore, fast particles with velocity on the order of $v = d/t = 3.9 \cdot 10^5\ m/s$ are the first to collide, in agreement with the early expansion dynamic observed for the single expanding plasma [11]. Light emission from the seeds strongly decreases yet after $t = 170$ ns, while the stagnation layer is still evolving. Its presence is clearly evident until some hundred of ns with a uniform particle distribution. Only at $t = 400$ ns a consistent decrease of emission is observed. For the thin foils a different dynamic is observed: figure 2 shows that the main plasma still expands on the front side of the target. However, at the rear side of the foil, a less intense but still significant emission is observed. Time resolved images reported in [3] show that at later expansion times, such as at $t = 160$ ns, emission of radiation is still observed from the stagnation layer and from the backward plasma. While seeds emission is almost totally disappeared. Thereafter the backward plasma evolves slowly in time together with the stagnation layer until $t \sim 510$ ns. The electrons composing the back-plasma evolve with a mean velocity of $2.27 \cdot 10^3\ m/s$. This velocity values was measured from TOF signals obtained by placing at the rear side of the foil a LP. The velocity is one order of magnitude lower than the typical velocity of laser plasmas obtained from the ablation of metal targets at similar laser fluences. Moreover the emission at the rear side of the foil was not observed as imaging, spectroscopy and LP measurements were realized in the emission region of the ions [3]. The singly charged ions composing the seeds are mostly forward peaked. Therefore the backward plasma is mainly composed of neutral atoms and slow expanding electrons [3].

4. Numerical Fusion Reaction Rate Calculations

Simulations are important to better understand the plume dynamic and to have a reliable theoretical model, for future reaction rate measurements, since the ES is not directly measurable. We implemented a hydrodynamic code called HYBLAS able to simulate and reproduce the experimental plume expansion a the laser irradiances of this work [13, 14]. HYBLAS uses an improved version of the Anisimov model [15]. In a laser energy regime up to $10^{11}\ Wcm^{-2}$ it can be used to simulate the adiabatic plasma expansion in terms of the time-varying plasma density and plasma temperature distribution. The Anisimov model solves the gas dynamical equations, under the basic hypothesis that the plasma expands selfsimilarly, adiabatically and isoentropically in vacuum. HYBLAS solves the equations of motion by adding two additional input parameters, in order to include the effect of the self-accelerating Coulombian Electric field and the difference between the ion and the electron temperature. The plasma evolution is strongly influenced by the charge separation of electrons and ions. In the separation layer a self-generated electric field arises to compensate the charge discrepancy. In a free flowing plasma the electric field boosts the plasma mobility. This field can be included with an additional Coulomb drift velocity term v_c in the dimensionless equation of motion [8]:

$$\xi_{shifted} = \xi + v_c = \xi + \sqrt{\frac{2 < z > eV_p}{M}} \frac{R_0}{t_0} \tag{4.1}$$

where $v_c = \frac{2 < z > eV_p}{M}$ is the contribution of the Coulomb shift to the velocity term, $< z >$ is the mean charge state, V_p is the plasma potential and M is the plume mass. The ion to electron

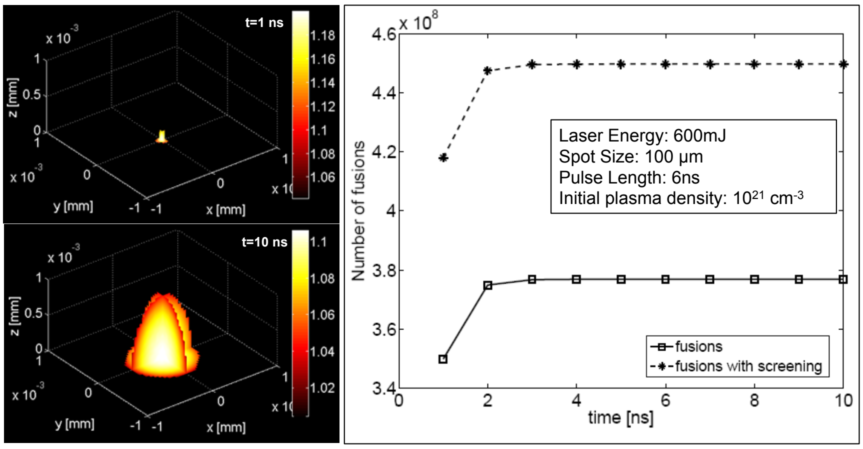

Figure 3: *Electron Screening at $t = 1$ ns and $t = 10$ ns (left) and total number of cumulated fusions after 24 hours of laser irradiance on a CD_2 target, evaluated with and without the influence of ES (right) [2].*

temperature ratio is given by the equation [8]:

$$\frac{k_B T_i}{kT_e} = \frac{1}{3}\left[\sqrt{\gamma} + \sqrt{2 < z >}\right]^2 \tag{4.2}$$

where γ is the adiabatic coefficient. This relation can be seen also as the temperature ratio dependence on a given charge state inside a single plume. It predicts not only that the ion temperature is consistently higher than the electron one, but also that the ratio grows with the charge state, that is in qualitative agreement with experimental results. With these "tricks" the model becomes like a two fluid approach and is able to well reproduce the experimental data. We refer to literature for the complete theoretical description of the code [8, 13]. The density and temperature mappings obtained from HYBLAS are then used to calculate the total number of fusions and to evaluate the influence of the ES. The fusion reaction rate was determined by applying the Gamow theory, using equation [1]:

$$R = \frac{1}{2} N < \sigma v > \int_0^{\infty} \rho(t) dt \tag{4.3}$$

where N is the total number of particles, $\rho(t)$ is the plasma density, and
$< \sigma v >$ is the reactivity, i.e the effectiveness of a fusion fuel given by the formula [1]:

$$< \sigma v > = \left(\frac{8}{\pi\mu}\right)^{\frac{1}{2}} \left(\frac{1}{kT_i}\right)^{\frac{3}{2}} \int_0^{\infty} \sigma(E) E \cdot exp\left(-\frac{E}{kT} - \frac{b}{\sqrt{E}}\right) dE \tag{4.4}$$

where T_i is the ion temperature, $\sigma(E)$ is obtained by the Gamow theory taking in account the tunnel effect of the nuclear coulomb barrier [1]. The electron screening was calculated according to the Debye-Huckel formula [2]:

$$U_e = exp\left(\frac{Z_1 Z_2 e^2}{k_B T \lambda_D}\right) \tag{4.5}$$

where Z_1 and Z_2 are the integral nuclear charges of the interacting particles and λ_D is the Debye lenght. A virtual CD_2 target was supposed to be irradiated for 24 hours at a laser peak irradiance of 10^{12} W/cm^2. In figure 3 the simulation results are reported. Figure 3 (left) shows the simulated

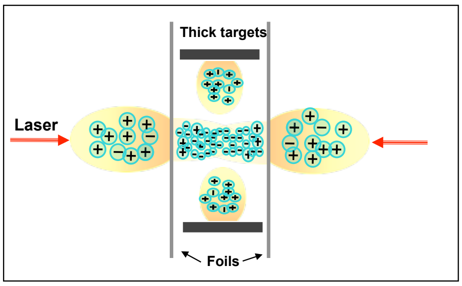

Figure 4: *Possible scheme of Backward Plumes Collision in order to study the Nuclear Screening.*

plume shape in terms of ES value at $t = 1$ ns and $t = 10$ ns of its expansion [2]. It is on the order of $1.2 - 1.1$ and remains almost constant during the plasma expansion. This occurs because the ES varies with ${\lambda_D}^{-1}$. i.e. with the ratio of the electron density and the electron temperature n_e/T_e. n_e and T_e both rapidly drop in time during plasma expansion with the same adiabatic trend [3]. Total number of fusions are reported in figure 3 (right) with and without the influence of the ES. Almost the totality of the fusion events takes place in the first $2-3$ ns after each laser pulse. We obtain about 430 and 520 fusion events per laser shot respectively without and with the influence of the ES. The ES has a weight of the 20% in determining the total number of fusions.

5. Final Discussion and Conclusions

The dynamic of the laser plasma develops among the classical adiabatic expansion from the influence of plasma instabilities. Instabilities are boosted by fast particles emission evolving at the early stage of the plume expansion. We observed fast electrons emitted with velocity up to $10^5 m/s$, followed by accelerated ion bunches of different charge states. DLs and MLs can develop, creating plasma instabilities, i.e self-generated electric fields where the quasi-neutrality of the plume is violated. An estimation of the fast peaks kinetic energies gives for the prompt electrons an energy of few $eV's$. The fast ions have an energy on the order of $KeV's$. Such instabilities affects the also the hydrodynamic expansion of the bulk plasma, that evolves as a TET plasma. The suppression of this non linear phenomena will be mandatory in future to avoid that plasma instabilities will affect the fusion reaction rate. Measurements on colliding plasmas confirmed that the electron density of the stagnation layer has a slower expansion dynamic in comparison to the single plume one. Fundamental were also the time resolved spectroscopy measurements reported in detail in [11]. They show that the seed density drops rapidly of one order of magnitude at about $t = 350$ ns with a trend typical of single LPP's. In contrast, the stagnation layer has a larger density that decreases with a longer delay time compared to the seed one: it *stagnates* for about 200 ns, from $t = 200-400$ ns [11]. At the same expansion times the stagnation layer has a lower temperature: it is on the order of $2-2.3eV$ (the seed has at comparable expansion times temperatures on the order of $2.8-3eV$). These conditions are of fundamental importance for future measurements of the ES, as this scales with the ratio of n_e/T_e. Measurements on thin foils confirmed the peculiar laser fluence regime: the main plasma is still forward peaked, but a slow back dynamic on the rear side of the target is observed. It appears that in this laser irradiance regime the intensity is not sufficient to produce a plasma that emerge entirely at the rear side of the foil [1]. This is not completely unexpected as in our case the energy transferred to the plasma, differs greatly with respect to the case of high intensity lasers and also encourages for future applications for ES studies. One future possible configuration could be the one reported in figure 4, where the collision of two backward expanding plasmas generated from thin foils interact with two forward colliding plasmas obtained from thick targets is studied. On the rear side of the foil one should be able to reproduce a rich cloud of cold electrons, that stagnate for very long times. It is expected, that due to the slow electron dynamic, collision will occur at larger times so that the particles reach the interaction front when they are cooled down. The collision of the two forward expanding plasmas will be used to obtain a not negligible number of fusions events. Preliminary numerical calculations confirmed that the calculated screening factor for LPP is very similar to the solar core one: it is on the order of 1.2, calculated with the typical plasma density and temperatures at laser irradiances of $10^{12}\ W/cm^2$ [2]. The overall collected data put in evidence that an experiment with a deuterated target, and 4π detectors for fusion products like neutrons, is physically meaningful. The forecasted experiment will give the opportunity to calculate the electron screening in a stellar-like environment. This will allow to test the validity of the classical Debye-Huckel theory and to evaluate the astrophysical factor. The experiment will be realized at energy domains on the order of hundreds of eV, never explored up to now in nuclear astrophysics [3, 2].

References

[1] E. Rolphs, *Cauldrons in Cosmos*, University of Chicago Press, 1998.

[2] D. Mascali et al., *Proceeding of IAU Symposium S274, Giardini Naxos, Italy*, **6**, (2011).

[3] N. Gambino, *Investigation of Laser Generated Plasmas for Astrophysical Applications*, PhD Thesis, University of Catania, 2011.

[4] B. Toftmann et al., *Phys. Rev. B*, **67**, (2003).

[5] S. Eliezer et al., *Phys. Report*, **172**, (1989).

[6] S. Amoruso et al., *Appl. Phys. Lett*, **75**, (1999).

[7] R. Isaac et al., *Appl. Phys. Lett* **73**, (1998).

[8] S. Tudisco et al., *Nucl. Instrum. A*, **653**, (2011).

[9] P. W. Rambo et al. *Phys. of Plasmas*, **12**, (1994).

[10] P. Hough et al. *J. of Phys. D: Appl. Phys.*, **42**, (2009).

[11] N. Gambino et al., *Appl. Surf. Science*, (2012), In press.

[12] N. Gambino et al., *Proc. of 37th EPS Conference on Plasma Physics, Dublin, Ireland*, (2010).

[13] N. Gambino et al. *IEEE Proc. of Animma Conference, Ghent, Belgium*, In press (2012).

[14] N. Gambino et al., *Rad. Eff. Def. in Solids*, **165**, (2010).

[15] S. Anisimov et al., *Phys. Rev. B*, **48**, (1993).

[16] M. Hegelich et al., *Phys. Rev. Lett.*, **89**, (2002).

[1] This dynamic arises at laser irradiances above $10^{12} W/cm^2$. It is studied for laser-plasma acceleration schemes [16]